# Interval-Analysis-Based Determination of the Singularity-free Workspace of Gough-Stewart Parallel Robots

M. Hadi Farzaneh Kaloorazi[1], Mehdi Tale Masouleh[2] and Stéphane Caro[3]

*Abstract*— **This paper proposes a systematic interval-based algorithm in order to obtain the maximal singularity-free sphere of 6-DOF parallel robots and as case study the 6-UPS parallel robot is considered. To this end, the main algorithm is divided into three sub-algorithms—for obtaining the constant-orientation workspace, the singularity loci and the maximal singularity-free workspace—which eases the understanding of the main approach and leads to a more effective and robust algorithm to solve the problem. The main contribution of this work can be regarded as the combination of the maximal singularity-free sphere with the workspace analysis as additional constraint to the problem.**

## I. Introduction

Parallel robots are wildly used in industrial fields, due to their host of advantages comparing with their counterparts, serial robots. parallel robots can tolerate heavier loads and exhibit a better rigidity. They are now the state-of-the-art of a wide range of commercial context, such as the Gough-Stewart platform [1] for flight simulator [2] and Delta robots [3] for pick an place applications. More details on the true origins of parallel robots is elaborated in [4] and [5]. However, there are some major drawbacks to wide spread of parallel robots in the industrial contexts, including, among others, mathematical complexities in analysing their kinematic properties and their limited workspace which is associated with uncontrollable situations, called singularity [6]. The kinematic analysis of parallel robots have stimulated the interest of many researchers to study their kinematic properties by proposing more efficient approaches. The forgoing approaches aim at refining the kinematic properties in order to obtain the most promising design [7]. The control of parallel robots leads inevitably to the solution of its Inverse and Forward Kinematic Problem (IKP and FKP). Due to the closed-loop nature of parallel robots, the FKP of parallel robots is usually a elegant task and was the central concern of many papers [8]. Since the limited workspace of parallel robots is coupled with singularities, in the design stage of a parallel robot the workspace and singularity analysis are of paramount importance and they should be analyzed in such a way that leads to a parallel robot with *singularity-free workspace* [9]. Emerging here is the notion of singularity of parallel robots in which the robot loses its inherent rigidity [10] and [11] and mathematically can be related to the regularity of some Jacobian matrix [12] and [6]. In fact, Jacobian matrices provide the mapping between the joint velocities and the Cartesian velocities of the robot which are arising from the first-order kinematic properties of the robot. In the literature, the singularity of parallel robots are classified upon different perspectives [13], and in this paper the one proposed in [6] is used whose perspective is perhaps the closest in spirit to the logic of this paper. Directly from [6], the singularities of parallel robots fall into three types: (1) Type I, inverse kinematic singularity, Type II direct kinematic singularity and Type III a combination of Type I and II. In the literature, the Type II singularities of parallel robots are the single most discussed one since are related to some non-linear expression and their investigation requires the usage of delicate techniques such as *screw theory* [14] and [5].

In what concerns the workspace of parallel robots, since generally their workspace is embedded into a six-dimensional space or 3-dimensional space accompanied with rotational motion, thus no visualization exists or which is extremely difficult to assess geometrically [15]. To circumvent the latter problems, sections with fixed translation or rotation of the complete workspace are proposed. The focus of this paper is on a commonly used such section: the constant-orientation workspace. The constant-orientation workspace consists of the set of feasible positions of the mobile platform for a prescribed orientation of the platform [15].

There has been an extensive study conducted on the singularity-free workspace of parallel robots where most of them are based on complicated numerical approaches and entail some limits. It is of paramount importance to study the singularity-free workspace of a parallel robot before going into the design stage and this can be exemplified by the number of the papers published on these issue. Bonev *et al.* in [14] conducted an exhaustive study on the singularity loci of planar 3-degree-of-freedom (DOF) parallel robots by resorting to screw theory. In [16], a method based on the geometrical parameters of the robot is proposed for which the singularity-free workspace of a three-legged parallel robot is obtained. Li *et al.* in [17] and [18], expressed mathematically the fact that the problem of singularity-free circle/sphere of 3 and 6-DOF parallel robots, as an optimization problem accompanied with a constraint and applied the Lagrangian multipliers to solve the problem. Jiang and Gosselin in [19]–[22] proposed some numerical recipes in order to find the singularity-free workspace of 3 and 6-DOF parallel robots. Recently, in [23], upon resorting to particle swarm optimization the singularity-free circle of a 3-DOF parallel robot was

[1]University of Tehran, Faculty of New Sciences and Technologies, North Kargar, Tehran, Iran, mhfarzane@ut.ac.ir

[2]University of Tehran, Faculty of New Sciences and Technologies, North Kargar, Tehran, Iran, m.t.masouleh@ut.ac.ir

[3]IRCCyN/CNRS, UMR 6597, 1 rue de la Noë, 44321 Nantes, France, stephane.caro@irccyn.ec-nantes.fr

obtained. Moreover, in [11], the problem of closeness to singularity is addressed by formulating the question in terms of constrained optimization problem.

This paper aims at establishing a systematic approach based on *interval analysis* [24]–[26] to obtain the Maximal Singularity-Free Sphere (MSFS) of general 6-DOF parallel robots. Two aspects which distinguish this work from others reported in the literature [9], [16]–[18], [23] are: (1) the center of the optimal sphere is not given from the outset and (2) the boundaries of the workspace are taken into account.

There are host of advantages relevant to using interval analysis as an alternative numerical method in order to obtain practically competent results for the singularity-free workspace of parallel robots and other kinematic properties [26] which can be summarized as follows [25]: (1) In contrast with many other intelligent mathematical tools which would result in a lengthy computation process and may converge to a local optimum, interval analysis is not a *black box*, since it requires to combine heuristics and numerical concepts to make it more effective, (2) It allows to find all the solutions with inequalities within a given search space [27]–[29], [29]–[31] (3) For two and three-dimensional problem it leads to see the evolution of the solutions and to monitor the procedure in order to have better insight into the problem and (4) it allows to take into account uncertainties in the model of the robot.

The remainder of the paper is organized as follows. First, the kinematic modelling of the robot under study, i.e., the so called 6-UPS parallel robot is broadly addressed. Then the general concept of interval analysis is presented. In Section III and IV, the proposed algorithm is fully explained and three *pseudo-codes* are provided to the end of better understanding the problem. Finally, some results are given which certify the effectiveness of the proposed algorithms.

## II. Review of Kinematic Properties, Inverse Kinematics, Singularity and Workspace

In this section, three important kinematic properties, namely IKP, singularity analysis and workspace are broadly reviewed. The IKP pertains to finding the values of joint variables for a given the position and orientation of the End-Effector (EE). Figure II represents a MSSM 6-UPS parallel robot. It should be noted that P stands for an actuated prismatic joint. In order to clearly establish the notation used here (inspired from [33]), consider a fixed coordinate frame $R : O - xyz$ attached to the base platform and a moving coordinate frame $R' : O' - x'y'z'$ attached to EE. Moreover, the $i^{\text{th}}$ leg is attached to the base platform at point $A_i$ and to EE at point $B_i$. Vectors $\mathbf{a}_i$ and $\mathbf{b}_i$, $i = 1, \ldots, 6$, are the positions of point $A_i$ and $B_i$, respectively. Furthermore, $\mathbf{Q}$ indicates the rotation matrix describing the rotation transformation from $R$ to $R'$, and $\rho_i$ is the joint variable of the $i^{\text{th}}$ prismatic joint. The position of point $O'$ with respect to the origin of the fixed coordinate can be written as:

$$[\mathbf{b}_i]_R = [\mathbf{r}]_R + \mathbf{Q}[\mathbf{b}_i]_{R'},\ i = 1, \ldots, 6 \tag{1}$$

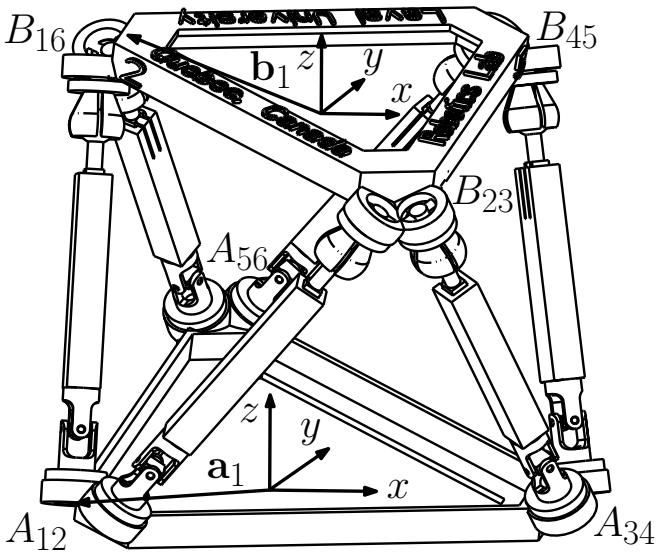


Fig. 1. The MSSM Gough-Stewart platform. The schematic is adapted from [32].

where $[\mathbf{r}]_R = [x_r, y_r, z_r]^T$ stands for the position vector of point $O'$ where the subscript $R$ indicates a fixed coordinate. Subtracting $\mathbf{a}_i$ from both sides of Eq. (1), leads to:

$$[\mathbf{b}_i - \mathbf{a}_i]_R = [\mathbf{r}]_R + \mathbf{Q}[\mathbf{b}_i]_{R'} - [\mathbf{a}_i]_R. \tag{2}$$

The left-side of Eq. (2) is clearly the vector connecting point $A_i$ to $B_i$, hence, by taking the Euclidean norm of each side, one can obtain the IKP of the $i^{\text{th}}$ limb as follows:

$$\rho_i = \| \ [\mathbf{b}_i - \mathbf{a}_i]_R \ \| = \| \ [\mathbf{r}]_R + \mathbf{Q}[\mathbf{b}_i]_{R'} - [\mathbf{a}_i]_R \ \|, \tag{3}$$

where $\| \cdot \|$ stands for the second Euclidean norm. Therefore, for a given robot, the actuator variable $\rho_i$ can be directly computed by having the position and orientation of EE.
In this paper, the actuation singularity, referred to as *Type II* [6], is more of concern which occurs when the moving platform possesses certain DOF after locking all the actuators. As a necessary condition, the rank of the actuated constraints system of parallel robot in a non-singular posture should be equal to six. Once it decreased, an infinitesimal motion can be observed on EE and the platform will be uncontrollable. Upon resorting screw theory, one can write kinematical screw system, $\$_i$, for a 6-UPS limb as:

$$\$_{\mathbf{i}} = \begin{bmatrix} \mathbf{e}_1^T & (\mathbf{a}_i \times \mathbf{e}_1)^T \\ \mathbf{e}_2^T & (\mathbf{a}_i \times \mathbf{e}_1)^T \\ \mathbf{0}^T & \mathbf{e}_{\rho_i}^T \\ \mathbf{e}_1^T & (\mathbf{b}_i \times \mathbf{e}_1)^T \\ \mathbf{e}_2^T & (\mathbf{b}_i \times \mathbf{e}_2)^T \\ \mathbf{e}_3^T & (\mathbf{b}_i \times \mathbf{e}_3)^T \end{bmatrix}, \quad i = 1, \ldots 6\,, \tag{4}$$

in which $\mathbf{e}_{\rho_i}$ stands for the direction of the $i^{\text{th}}$ prismatic joint. From Eq. (4), it can be concluded that, no constraint wrench is imposed by the limb to the EE, therefore the robot under study has 6-DOF. Furthermore, from the above it follows

TABLE I

PSEUDO-CODE OF ALG. A FOR OBTAINING THE REGION DEFINED BY $\mathfrak{M}(\cdot)$ FOR 6-UPS PARALLEL ROBOTS.

- **Initialize** list $\mathcal{L}$ containing initial task space interval (box)
- **Initialize** empty lists $\mathcal{L}_{\text{in}}$, $\mathcal{L}_{\text{out}}$ and $\mathcal{L}_b$
- **Initialize** $\mathsf{B_C}$ as the current box
- **Module** $\mathfrak{M}(\cdot)$
- **While** ($\mathcal{L}$ is not empty)
  - **Extract** first column of matrix $\mathcal{L}$ and **copy** it to $\mathsf{B_C}$
  - **Empty** first column of $\mathcal{L}$
  - **Case** $\mathsf{B_C}$ is inner, outer or boundary box
    - **Case 1:** $\mathfrak{M}(\mathsf{B_C}) == 1$ ($\mathsf{B_C}$ is inside the *region*)
      **Add** $\mathsf{B_C}$ at the end of list $\mathcal{L}_{\text{in}}$
    - **Case 2:** $\mathfrak{M}(\mathsf{B_C}) == -1$ ($\mathsf{B_C}$ is outside the *region*)
      **Add** $\mathsf{B_C}$ at the end of list $\mathcal{L}_{\text{out}}$
    - **Case 3:** $\mathfrak{M}(\mathsf{B_C}) == 0$ ($\mathsf{B_C}$ lies within boundary of *region*)
      **If** (dimension of $\mathsf{B_C} > \epsilon$)
      **Bisect** $\mathsf{B_C}$ by the biggest edge
      **Add** two new boxes at the end of list $\mathcal{L}$
      **Else If** (threshold dimension $\epsilon$ has been reached)
      **Add** $\mathsf{B_C}$ at the end of list $\mathcal{L}_b$
      **End If**
  - **End Case**
- **End While**
- **Return** $\mathcal{L}_b$ as the *region* boundaries

that the Jacobian matrix of actuated constraints system of a 6-UPS robot can be written as:

$$\mathbf{J} = \begin{bmatrix} \mathbf{e}_{\rho_1}^T & (\mathbf{b}_1 \times \mathbf{e}_{\rho_1})^T \\ \mathbf{e}_{\rho_2}^T & (\mathbf{b}_2 \times \mathbf{e}_{\rho_2})^T \\ \mathbf{e}_{\rho_3}^T & (\mathbf{b}_3 \times \mathbf{e}_{\rho_3})^T \\ \mathbf{e}_{\rho_4}^T & (\mathbf{b}_4 \times \mathbf{e}_{\rho_4})^T \\ \mathbf{e}_{\rho_5}^T & (\mathbf{b}_5 \times \mathbf{e}_{\rho_5})^T \\ \mathbf{e}_{\rho_6}^T & (\mathbf{b}_6 \times \mathbf{e}_{\rho_6})^T \end{bmatrix}. \tag{5}$$

Each row of the Jacobian matrix is a Plüker line which is reciprocal to all the passive joints of the corresponding limb. $\det(\mathbf{J}) = 0$ represents the singularity loci of the robot and will be used in section III, in order to determine singularity loci of the robot.

The workspace of a robot consists set of Cartesian points for which the EE is able to reach them. The solution of the IKP can be used to obtain the workspace of the robot for a given mechanical stroke associated to each limb, $\rho_{\min} < \rho_i < \rho_{\max}$. Hence, each point of the Cartesian space which satisfies Eq. (3) for the given stroke, is a member of the workspace. Furthermore, the workspace of a 6-UPS parallel robot is the common area of the intersection of six inner and six outer spheres, known as vertex space.

## III. INTERVAL-BASED ALGORITHM FOR WORKSPACE AND SINGULARITY LOCI DETERMINATION (ALG. A)

Interval-based solvers can solve system of numerical equation such as non-linear equations or inequalities. One of the main advantages of interval analysis is to prevent round-off errors [24]. Moreover, interval analysis presents a graphical performance and certainty of obtained solutions. An interval variable $X$ is shown as $X = [\underline{X}, \overline{X}]$ in which $\texttt{inf}(X) = \underline{X}$ is the lower bound of the interval and $\texttt{sup}(X) = \overline{X}$ is the upper bound.

TABLE II

PSEUDO-CODE OF ALG. B IN ORDER TO OBTAIN THE MSFS FOR 6-UPS PARALLEL ROBOTS FOR AN GIVEN INITIAL GUESS BOX.

- **Input** list $\mathcal{B}$ containing boundaries such as workspace borders and singularity borders (taken from Alg. A, Table (I))
- **Initialize** box $\mathsf{B_i}$ as initial guess, defined by the user
- **Substitute** $\mathsf{B_C} \leftarrow \mathsf{B_i}$
- **While** (dimension $\mathsf{B_C} > \epsilon$)
  - **Bisect** $\mathsf{B_C}$ by the biggest edge into $\mathsf{B_{C1}}$ and $\mathsf{B_{C2}}$
  - **Calculate** distance from $\mathsf{B_{C1}}$ and then $\mathsf{B_{C2}}$ to $\mathcal{B}$, with respect to Eq. (6) results $\mathbf{D_{C1}}$ and $\mathbf{D_{C2}}$
  - **If** ($\mathbf{min}(\mathbf{D_{C1}}) > \mathbf{min}(\mathbf{D_{C2}})$)
    **Subs** $\mathsf{B_{C1}}$ into the box $\mathsf{B_C}$
    $\mathbf{D} \leftarrow \mathbf{D_{C1}}$
    **Else**
    **Subs** $\mathsf{B_{C2}}$ into the box $\mathsf{B_C}$
    $\mathbf{D} \leftarrow \mathbf{D_{C2}}$
    **End If**
  - **End While**
- **Return** $C_0 \leftarrow$ **Center**($\mathsf{B_C}$), as MSFC center
- **Return** $r_0 \leftarrow$ **min**($\mathbf{D}$), as MSFC radius

In this section, an interval-based algorithm is introduced to the end of finding the workspace and the singularity loci. This algorithm, called Alg. A, is based on a *Branch & Prune* procedure [25]. Table I indicates the reasoning of Alg. A. A set of interval values is called *box* which, in a constant-orientation-workspace, represent a three-dimensional box and consists of $x$, $y$ and $z$. In Alg. A, module $\mathfrak{M}(\mathsf{B})$ checks each current box, $\mathsf{B_C}$, and returns three probable conditions as below:

- 1: if box $\mathsf{B_C}$ is fully inside the region ($\texttt{inf}(\mathsf{R_C}) > 0$)
- -1: if box $\mathsf{B_C}$ is fully outside the region ($\texttt{sup}(\mathsf{R_C}) < 0$)
- 0: otherwise i.e, parts of $\mathsf{B_C}$ may be either inside or outside the region ($\texttt{inf}(\mathsf{R_C}) \cdot \texttt{sup}(\mathsf{R_C}) < 0$).

Here and throughout this paper, the term *region* could be either the constant-orientation workspace, Eq. (3), or the singularity loci, $\det(\mathbf{J}) = 0$, and Alg. A could be applied to both of them. $\mathsf{R_C}$ is the result of applying $\mathsf{B_C}$ into corresponding equations. If $\mathfrak{M}(\mathsf{B})$ returns 1 or -1, then box $\mathsf{B}$ will be eliminated from branch & prune procedure and if it returns 0, then $\mathsf{B}$ will get bisected and two new boxes will be checked individually latter. If the desired accuracy $\epsilon$ is reached, then the algorithm stops and the boundaries of *region* is obtained.

In Table I, first of all, in order to store obtained results, four lists are initialized as follows: $\mathcal{L}$ for undecided boxes, $\mathcal{L}_{in}$ for boxes inside of the *region*, $\mathcal{L}_{out}$ outside of the *region* and $\mathcal{L}_b$ for the borders of the *region*. In Table I, in each iteration, between **while** and **end while**, the procedure extracts first column of list $\mathcal{L}$ which consists of a three-dimensional box and substitutes it into the current box $\mathsf{B_C}$. Then the first column of $\mathcal{L}$ must be eliminated. This action prevents computer memory of being overloaded. Applying $\mathsf{B_C}$ into corresponding equations, Eq. (3) for the constant-orientation workspace and $\det(\mathbf{J}) = 0$ for the singularity loci, module $\mathfrak{M}$ results one of the cases discussed latter. If $\mathfrak{M}(\mathsf{B_C})$ returns 0 and threshold $\epsilon$ is not reached, then Alg. A continue, otherwise it stops. Finally, boundaries of

TABLE III

PSEUDO-CODE FOR ALG. C TO OBTAIN THE IMPROVED MSFS OF 6-UPS PARALLEL ROBOTS.

- **Run** algorithm B (Table II) Consider initial guess $\mathsf{B_i}$ and point $C_i$
- $i \leftarrow 0$
- **While** ($C_i$ is not close to the edges of $\mathsf{B_i}$)
  - **Create** box $\mathsf{B_i}$ with $C_0$ as center point and **dimension**($\mathsf{B_0}$)
  - **Run** algorithm B (Table II)
  - $i \leftarrow i + 1$

  **End While**
- **Return** $C_i \equiv C_f$ as MSFC center
- **Return** $r_i \equiv r_f$ as MSFC radius

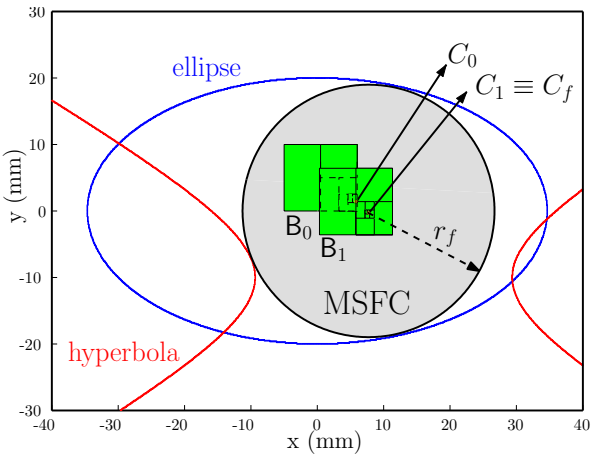


Fig. 2. Result of applying Alg. B and C in order to find maximal embedded circle in common area of intersection of an ellipse (i.e. workspace) and a hyperbola (i.e. singularity loci). In Alg. B, initial guess box $\mathsf{B_0}$ found $C_0$ which is close to the border of $\mathsf{B_0}$. Hence, in Alg. C, another guess box, $\mathsf{B_1}$, is created and point $C_1$ is obtained which is the center point of MSFC

the workspace and the singularity loci will be stored in $\mathcal{L}_b$.

## IV. ALGORITHMS FOR OBTAINING THE MAXIMAL SINGULARITY-FREE SPHERE IN THE WORKSPACE OF PARALLEL ROBOTS (ALG. B AND C)

Reaching this step, from Alg. A the boundaries of workspace and singularity loci an be obtained. In this section, two algorithms are introduced in order to obtain the center point of MSFS. First, a sub-routine, called Alg. B (Table II), is explained to the end of finding a proper candidate of being the center point of MSFS. If the obtained point does not satisfy necessary conditions, then a second sub-routine, called Alg. C (Table III), will continue the procedure until the certain center point of MSFS is found.

For the sake of simplicity, a representative example, Fig. (2) is perused for Alg. B and C. Consider an ellipse (as a representation of the workspace) and a hyperbola (as a representation of the singularity loci) in two-dimensional Cartesian plane, represented in Fig. 2, in which, the maximal embedded circle (Maximal Singularity-Free Circle, MSFC) in common area of their intersection, should be obtained. First of all, using Alg. A, the interval-based borders of the ellipse and the hyperbola can be obtained. Note that these borders consist of a set of small boxes which have the dimension lower than $\epsilon$. Information given to Alg. B in order to obtain the the center point of the MSFC/MSFS ($C_f$) are of two sort:(1) the set of boundary boxes obtained by Alg. A and (2) an initial guess box, prescribed by user ($\mathsf{B_0}$). This initial guess box can be located anywhere and it could be one of the boxes inside the list $\mathcal{L}_{in}$ achieved in Alg. A. The first step in Alg. B consists in initializing box $\mathsf{B_0}$ and substitutes it into the current box $\mathsf{B_C}$. Then, bisecting $\mathsf{B_0}$ by the largest edge (Table II). Consequently, it returns two new boxes ($\mathsf{B_{C1}}$ and $\mathsf{B_{C2}}$). Then the algorithm calculates the corresponding distance of $\mathsf{B_{C1}}$ and $\mathsf{B_{C2}}$ to the set of workspace and singularity interval-boundaries ($\mathcal{B}$) separately, using Eq. (6).

$$\mathbf{D}_{\mathsf{C}j} = \|\mathsf{B}_{\mathsf{C}j} - \mathcal{B}\| \quad j = 1, 2\ , \tag{6}$$

in which $\mathbf{D}_{\mathsf{C}j}$ is the distance $\mathsf{B}_{\mathsf{C}j}$ to $\mathcal{B}$. It should be noted that $\mathbf{D}_{\mathsf{C}j}$ is an interval value. Between $\mathsf{B_{C1}}$ and $\mathsf{B_{C2}}$, the one with the greater lower bound, is kept for further operations and substituted into $\mathsf{B_C}$ and the other one is ignored. Then, new $\mathsf{B_C}$ is bisected and the procedure continues until the desired accuracy, $\epsilon$, is reached which leads to a small box and with an acceptable approximation it could be regarded as a point, $C_0$. This point could be an appropriated candidate of being the center point of MSFC/MSFS. Algorithm B returns $C_0$ as the center point and $r_0 = \texttt{inf}(\mathbf{D})$ as the radius of MSFC/MSFS. A necessary condition is that $C_0$ is not close to the edges of $\mathsf{B_0}$, where this closeness must be more than $\epsilon$. If $C_0$ is close to the edges of $\mathsf{B_0}$, meaning that the center point tends to travel through the singularity-free workspace. The second subroutine consists in obtaining a center point which is not close to the edges of the guess box. To do so, Alg. C checks if point $C_0$ is close to the edges of $\mathsf{B_0}$, then creates another guess box, $\mathsf{B_1}$ around $C_0$ with the same size as $\mathsf{B_0}$. Algorithm B will be repeated for the new guess boxes $\mathsf{B_i}$, $i = 1, 2 \ldots n$ until the center point obtained is not close to the edge of last guess box. The obtained point, $C_f$, is the center point of MSFC/MSFS and the radius of circle/sphere can be computed by calculating the distance of this point to the set of boundaries, $r_f$.

## V. RESULTS

In order to have a better insight into the reasoning of all algorithms proposed in this paper, this section is devoted entirely to analysis the obtained solutions from algorithms A, B and C for a 6-UPS parallel robot with design parameters as given in Table IV.

Figures 3(a) and 3(b) represent both the constant-orientation-workspace for $\theta = 0$, $\phi = 0$, $\psi = 0$ and $z = [510, 530]$, obtained by a CAD software and Alg. A, respectively. In turn, for the same set of orientations used for Fig. 3, Fig. 4(a) and 4(b) represent respectively the implicit and interval-based (Alg. A) representations of the singularity loci of the parallel robot under study.

Moreover, as it can be observed from Fig. 5, the MSFS is tangent to both singularity loci and workspace boundaries. By inspection, it can be inferred that the obtained MSFS corresponds to the optimal inscribed sphere bounded by the workspace and the singularity loci.

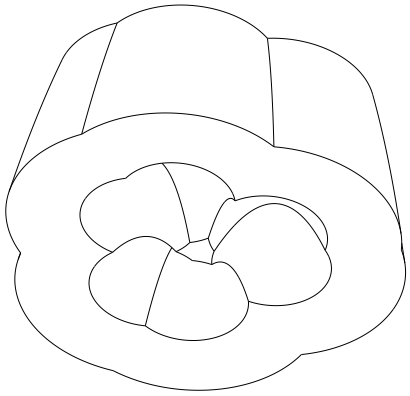

(a) Intersection of six inner and six outer spheres, obtained from a CAD software

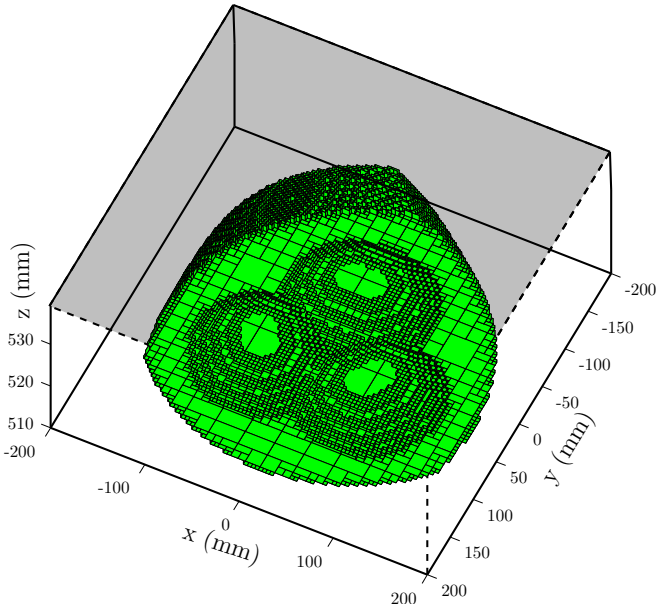


(b) The constant-orientation workspace of 6-UPS parallel robot with geometry mentioned in Table IV, section of $z$=510...530

Fig. 3. The constant-orientation workspace of 6-UPS parallel robot with design properties as given in Table IV.

For the sake of better understanding, Fig. 6 represents a cross-sectional view of the result depicted in Fig. 5. It is worth mentioning that, in Fig. 6, the gray circles are cross-section views of the MSFS in different $xy$-planes. As it can be observed from the forgoing figure, the gray circles are neither tangent to the workspace boundaries nor to the singularity loci. The latter statement is not in contrary to the fact that the MSFS should absolutely be tangent to the constraint of the problem, since this takes place in 3-dimensional space to a set of points non lying in the prescribed cross-sectional planes along the $z$-axis.

TABLE IV

GEOMETRIC PARAMETERS OF THE 6-UPS PARALLEL ROBOT UNDER STUDY (ALL LENGTHS ARE GIVEN IN *mm*).

| i | 1 | 2 | 3 | 4 | 5 | 6 |
|---|---|---|---|---|---|---|
| $x_{ai}$ | 92.58 | 132.58 | 40.00 | -40.00 | -132.58 | -92.58 |
| $y_{ai}$ | 99.64 | 30.36 | -130.00 | -130.00 | 30.36 | 99.64 |
| $z_{ai}$ | 23.10 | 23.10 | 23.10 | 23.10 | 23.10 | 23.10 |
| $x_{bi}$ | 30.00 | 78.22 | 48.22 | -48.22 | -78.22 | -30.00 |
| $y_{bi}$ | 73.00 | -10.52 | -62.48 | -62.48 | -10.52 | 73.00 |
| $z_{bi}$ | -37.10 | -37.10 | -37.10 | -37.10 | -37.10 | -37.10 |
| $\rho_{i_{\min}}$ | 454.5 | 454.5 | 454.5 | 454.5 | 454.5 | 454.5 |
| $\rho_{i_{\max}}$ | 504.5 | 504.5 | 504.5 | 504.5 | 504.5 | 504.5 |

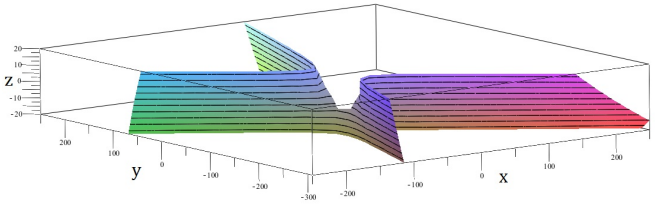


(a) Implicit representation of the singularity loci of a 6-UPS parallel robot

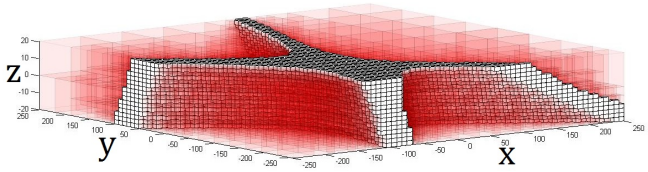


(b) Singularity loci surface of a 6-UPS parallel robot, obtained from Alg. A. The set of white boxes are outside of the singularity loci and red-transparent boxes lie on the singularity loci

Fig. 4. Singularity loci of 6-UPS parallel robot with design properties as given in Table IV (a) implicitly depicted (b) interval-based

## VI. CONCLUSION

This paper presented three interval-based algorithms, called A, B and C, in order to obtain respectively the constant-orientation workspace, the singularity, the maximal singularity-free workspace for a given box and the maximal singularity-free workspace for the entire workspace of 6-DOF parallel robot and as case study the MSSM Gough-Stewart platform, 6-UPS, parallel robot is considered. The proposed algorithm laid down the state-of-the-art for formulating the problem of finding the maximal singularity-free workspace of 6-DOF parallel robots. However, it could be readily extended to other robots, and open an avenue to find a systematic approach to do so. The results obtained from these algorithms revealed that the proposed algorithms are robust and could be also use to the optimum synthesis of the robots under study. Ongoing works include the extension of the proposed algorithm to more complex parallel robots.

## REFERENCES

[1] B. Dasgupta and T. Mruthyunjaya, "The Stewart Platform Manipulator: A Review," *Mechanism and Machine Theory*, vol. 35, no. 1, pp. 15–40, 2000.

[2] D. Stewart, "A Platform with Six Degrees of Freedom," vol. 180, no. 1. Sage Publications, 1965, pp. 371–386.

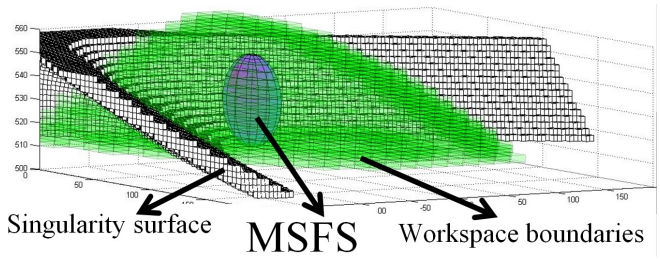


Fig. 5. The MSFS of 6-UPS parallel robot for $\theta = 0$, $\phi = 0$, $\psi = 0$ and $z = [510, 530]$. The set of white boxes represent singularity surface and green-transparent boxes are inside the constant-orientation-workspace. MSFS is obtained in such a way that is tangent to both the singularity surface and the workspace.

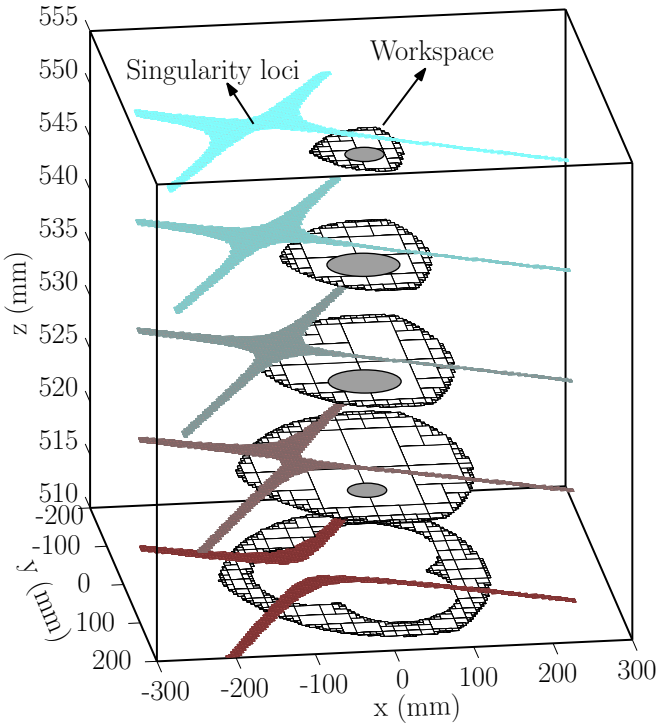


Fig. 6. Interval-based results for the MSFS for $\theta = 0$, $\phi = 0$, and $\psi = 0$. To not overload the figure, only cross-sectional plan are considered to represent the constant-orientation workspace and the singularity loci. The gray circles represent sections of the MSFS.


[3] R. Clavel, "Delta, a fast robot with parallel geometry," in *Proceedings of the 18th International Symposium on Industrial Robots*, 1988, pp. 91–100.

[4] "Parallelmic, http://www.parallemic.org/."

[5] X. Kong and C. Gosselin, *Type Synthesis of Parallel Mechanisms*. Springer, Heidelberg, 2007, vol. 33.

[6] C. Gosselin and J. Angeles, "Singularity Analysis of Closed-Loop Kinematic Chains," *IEEE Transactions on Robotics and Automation*, vol. 6, no. 3, pp. 281–290, 1990.

[7] M. Saadatzi, M. Tale Masouleh, H. Taghirad, C. Gosselin, and P. Cardou, "On the Optimum Design of 3-RPR Parallel Mechanisms," in *19th Iranian Conference on Electrical Engineering (ICEE)*. IEEE, 2011, pp. 1–6.

[8] J. Merlet, "Direct Kinematics of Planar Parallel Manipulators," in *IEEE International Conference on Robotics and Automation*, vol. 4. IEEE, 1996, pp. 3744–3749.

[9] M. Tale Masouleh and C. Gosselin, "Determination of Singularity-free Zones in the Workspace of Planar 3-PRR Parallel Mechanisms," *Journal of Mechanical Design*, vol. 129, p. 649, 2007.

[10] J. P. Merlet, *Parallel Robots*. Springer, 2006.

[11] P. Voglewede and I. Ebert-Uphoff, "Overarching Framework for Measuring Closeness to Singularities of Parallel Manipulators," *IEEE Transactions on Robotics*, vol. 21, no. 6, pp. 1037–1045, 2005.

[12] J. Merlet and P. Donelan, "On the Regularity of the Inverse Jacobian of Parallel Robots," *Advances in Robot Kinematics*, pp. 41–48, 2006.

[13] M. Conconi and M. Carricato, "A New Assessment of Singularities of Parallel Kinematic Chains," *IEEE Transactions on Robotics*, vol. 25, no. 4, pp. 757–770, 2009.

[14] I. A. Bonev, D. Zlatanov, and C. M. Gosselin, "Singularity Analysis of 3-DOF Planar Parallel Mechanisms Via Screw Theory," *Journal of Mechanical Design*, vol. 125, p. 573, 2003.

[15] M. Saadatzi, M. Tale Masouleh, and H. Taghirad, "Workspace Analysis of 5-PRUR Parallel Mechanisms (3T2R)," *Robotics and Computer-Integrated Manufacturing*, 2012.

[16] Y. Yang and J. O'Brien, "A Case Study of Planar 3-RPR Parallel Robot Singularity Free Workspace Design," in *International Conference on Mechatronics and Automation (ICMA)*. IEEE, 2007, pp. 1834–1838.

[17] H. Li, C. Gosselin, and M. Richard, "Determination of Maximal Singularity-free Zones in the Workspace of Planar Three-degree-of-freedom Parallel Mechanisms," *Mechanism and machine theory*, vol. 41, no. 10, pp. 1157–1167, 2006.

[18] H. Li, C. Gosselin, and R. M.J, "Determination of the Maximal Singularity-free Zones in the Six-dimensional Workspace of the General Gough-Stewart Platform," *Mechanism and machine theory*, vol. 42, no. 4, pp. 497–511, 2007.

[19] Q. Jiang and G. C.M., "Geometric Synthesis of Planar 3-RPR Parallel Mechanisms for Singularity-free workspace," *Transactions of the Canadian Society for Mechanical Engineering*, vol. 33, no. 4, pp. 667–678, 2009.

[20] Q. Jiang and C. Gosselin, "The Maximal Singularity-Free Workspace of Planar 3-RPR Parallel Mechanisms," in *Proceedings of the 2006 International Conference on Mechatronics and Automation*. IEEE, 2006, pp. 142–146.

[21] L. Jiang, "Singularity-Free Workspace Analysis and Geometric Optimization of Parallel Mechanisms," Ph.D. dissertation, Laval University, Quebec, QC, Canada, june 2008.

[22] Jiang and Gosselin, "Geometric Optimization of Planar 3-RPR Parallel Mechanisms," *Transactions of the Canadian Society for Mechanical Engineering*, vol. 31, no. 4, pp. 457–468, 2007.

[23] G. Abbasnejad, H. Daniali, and S. Kazemi, "A New Approach to Determine the Maximal Singularity-free Zone of 3-RPR Planar Parallel Manipulator," *Robotica*, vol. 1, no. 1, pp. 1–8.

[24] R. Moore and F. Bierbaum, *Methods and Applications of Interval Analysis*. Society for Industrial Mathematics, 1979, vol. 2.

[25] J. Merlet, "Interval Analysis and Robotics," *Robotics Research*, pp. 147–156, 2011.

[26] F. Hao and J. Merlet, "Multi-criteria Optimal Design of Parallel Manipulators Based on Interval Analysis," *Mechanism and Machine Theory*, vol. 40, no. 2, pp. 157–171, 2005.

[27] Merlet, "Solving the Forward Kinematics of a Gough-type Parallel Manipulator with Interval Analysis," *The International Journal of robotics research*, vol. 23, no. 3, pp. 221–235, 2004.

[28] D. Oetomo, D. Daney, B. Shirinzadeh, and J. Merlet, "Certified Workspace Analysis of 3RRR Planar Parallel Flexure Mechanism," in *IEEE International Conference on Robotics and Automation (ICRA)*. IEEE, 2008, pp. 3838–3843.

[29] D. Chablat, P. Wenger, F. Majou, and J. Merlet, "An interval analysis based study for the design and the comparison of three-degrees-of-freedom parallel kinematic machines," *The International Journal of Robotics Research*, vol. 23, no. 6, pp. 615–624, 2004.

[30] E. Hansen and S. Sengupta, "Global constrained optimization using interval analysis," *Interval Mathematics*, vol. 1980, pp. 25–47, 1980.

[31] E. Hansen and G. Walster, *Global optimization using interval analysis: revised and expanded*. CRC, 2003, vol. 264.

[32] Laboratoire de Robotique de L'Université Laval. [Online]. Available: http://www.robot.gmc.ulaval.ca

[33] C. Gosselin, "Determination of the Workspace of 6-DOF Parallel Manipulators," *ASME Journal of Mechanical Design*, vol. 112, no. 3, pp. 331–336, 1990.